The Novel Neutrophil Differentiation Marker Phosphatidylglucoside Mediates Neutrophil Apoptosis

Katsunari Kina,* Hiromi Masuda,* Hitoshi Nakayama,† Yasuko Nagatsuka,‡ Takuji Nabetani,‡ Yoshio Hirabayashi,‡ Yasue Takahashi,§ Kazunori Shimada,§ Hiroyuki Daida,§ Hideoki Ogawa,* Kenji Takamori,* and Kazuhisa Iwabuchi*,†

A new type of glycolipid, phosphatidylglucoside (PtdGlc), was identified as a component of raft-like membrane domains of the human leukemia cell line HL-60. In this study, we show that PtdGlc forms functional domains that are different from those produced by lactosylceramide (LacCer)-enriched lipid rafts. These rafts initiate neutrophil apoptosis. Neutrophils are the only type of human peripheral blood leukocyte or monocyte-derived dendritic cell to express large amounts of PtdGlc on their cell surfaces. PtdGlc was not colocalized with LacCer. Anti-PtdGlc IgM DIM21 did not induce neutrophil chemotaxis or superoxide generation, whereas anti-LacCer IgM T5A7 induced these activities. DIM21, but not T5A7, significantly induced neutrophil apoptosis. DIM21-induced apoptosis was inhibited by specific inhibitors of cysteine-containing aspartate-specific proteases (caspases)-8, -9, and -3 but not by the Src family kinase inhibitor PP1, PIP_3 kinase inhibitor LY294002, NADPH oxidase inhibitor diphenyleneiodonium, superoxide dismutase, or catalase. PtdGlc was colocalized with Fas on the neutrophil plasma membrane. DIM21 and the agonist anti-Fas Ab DX2 induced the formation of large Fas-colocalized clusters of PtdGlc on the plasma membrane. Furthermore, the antagonistic anti-Fas Ab ZB4 significantly inhibited DIM21-induced neutrophil apoptosis. These results suggest that PtdGlc is specifically expressed on neutrophils and mediates apoptosis of these cells, and that the Fas-associated death signal may be involved in PtdGlc-mediated apoptosis. ***The Journal of Immunology*****, 2011, 186: 5323–5332.**

Polymorphonuclear neutrophils play critical roles in the innate immune system by recognizing pathogen-associated molecular patterns via pattern recognition receptors expressed on the cell surface and then phagocytosing and eliminating microorganisms (1). Neutrophils have a very short lifespan and undergo apoptosis within 24–48 h after leaving the bone marrow. Apoptosis is the major mechanism for limiting neutrophil numbers in vivo and is important in the clearance of neutrophils from inflamed tissues by tissue macrophages, which is critical for limiting inflammatory tissue injury and the subsequent resolution of inflammation (2–4).

Membrane microdomains/lipid rafts are involved in the innate immune responses and apoptosis of neutrophils (5–8). Lipid rafts are functional lipid domains enriched with glycosphingolipids, GPI-anchored proteins, cholesterol, and signal-transduction molecules, including Src family kinases and trimeric G proteins (9). The neutral glycosphingolipid lactosylceramide (LacCer, CDw17; Galβ4Glcβ1Cer) is the most abundant glycosphingolipid in human neutrophils and acts as a pattern recognition receptor in these cells (5, 6, 10–12). LacCer forms lipid rafts on the plasma membranes of neutrophils in combination with the Src family kinase Lyn (5, 6). These LacCer-enriched lipid rafts are involved in neutrophil chemotaxis (8), phagocytosis (6), and the generation of superoxide (5). Although the fatty acid chain structures of LacCer are highly variable, the presence of a C24:0 or C24:1 fatty acid chain in LacCer is necessary for its functional connection with Lyn in lipid rafts of HL-60 cells (6).

Phosphatidylglucoside (PtdGlc) is a unique cell-surface glycophospholipid that was originally found in human umbilical cord RBCs (13). PtdGlc is recovered in the Triton X-100–insoluble fraction after sucrose density-gradient ultracentrifugation, suggesting that PtdGlc forms raft-like membrane domains (9, 14–16). PtdGlc plays a role in differentiation events, which may be initiated at specific lipid domains on the cell surface. For example, treatment of HL-60 cells with the recombinant anti-PtdGlc Fab Ab rGL-7 induces differentiation of HL-60 cells into neutrophilic cells. PtdGlc forms lipid rafts on the plasma membrane (15, 16), because it consists exclusively of saturated fatty acid chains C18:0 and C20:0 at the sn-1 and sn-2 positions of the glycerol backbone, respectively (17). Treatment with anti-PtdGlc Ab induces phos-

*Institute for Environmental and Gender-Specific Medicine, Juntendo University School of Medicine, Urayasu-shi, 279-0021 Chiba, Japan; †Laboratory of Biochemistry, Juntendo University School of Health Care and Nursing, Urayasu-shi, 279-0023 Chiba, Japan; ‡Laboratory for Molecular Membrane Neuroscience, RIKEN Brain Science Institute, Wako-shi, 351-0198 Saitama, Japan; and §Department of Cardiovascular Medicine, Juntendo University School of Medicine, Bunkyo-ku, 113-0124, Tokyo, Japan

Received for publication June 23, 2010. Accepted for publication February 11, 2011.

This work was supported in part by the Mizutani Foundation for Glycoscience (to K.I.), the Hamaguchi Foundation for the Advancement of Biochemistry (to K.I.), the "High-Tech Research Center" Project for Private Universities matching fund subsidy, and by Grant-in-Aid S0991013 from the Foundation of Strategic Research Projects in Private Universities from the Ministry of Education, Culture, Sport, Science, and Technology, Japan.

K.K., H.M., and H.N. performed experiments; Y.N. provided Abs and performed mass spectrometry analysis; T.N. performed mass spectrometry analysis; Y.H. provided Abs and analyzed data; Y.T., K.S., and H.D. performed flow cytometric analysis; H.O. and K.T. analyzed data; and K.I. designed and performed experiments.

Address correspondence and reprint requests to Dr. Kazuhisa Iwabuchi, Institute for Environmental and Gender-Specific Medicine, Juntendo University Graduate School of Medicine, 2-1-1 Tomioka Urayasu-shi, Chiba 279-0021, Japan. E-mail address: iwabuchi@juntendo.ac.jp

The online version of this article contains supplemental material.

Abbreviations used in this article: Alexa Fluor 488-DIM21, Alexa Fluor 488-conjugated DIM21; Alexa Fluor 647-T5A7, Alexa Fluor 647-conjugated T5A7; C/M, chloroform/methanol; DC, dendritic cell; DIC, differential interference contrast; DMEM/F12-BSA, DMEM/F12 medium supplemented with 1 mg/ml BSA; DMEM/F12-FBS, DMEM/F12 medium supplemented with 10% FBS; DPI, diphenyleneiodonium; LacCer, lactosylceramide; LC/MS/MS, liquid chromatography-tandem mass spectrometry; MS, mass spectrometry; PI, propidium iodide; PLP, periodate-lysine paraformaldehyde; PtdGlc, phosphatidylglucoside; ROS, reactive oxygen species; SOD, superoxide dismutase.

www.jimmunol.org/cgi/doi/10.4049/jimmunol.1002100

phorylation of Lyn and Hck. Reduction of endogenous cholesterol with methyl–β-cyclodextrin suppresses anti-PtdGlc Ab-stimulated tyrosine phosphorylation, resulting in the up- and downregulation of CD38 and c-Myc expression, respectively (16). Therefore, PtdGlc may form functional raft-like domains on the plasma membranes of HL-60 cells, although it does not have C24 fatty acid chains (17). PtdGlc forms distinct lipid domains from sphingolipids on the outer leaflet of the plasma membrane of HL-60 cells (18). These observations suggest that PtdGlc and LacCer form distinct lipid domains on the plasma membrane and mediate cell functions via different signaling mechanisms.

This study demonstrated that PtdGlc is highly expressed on human neutrophils and is located in lipid domains distinct from LacCer-enriched lipid rafts in these cells. In addition, PtdGlc, but not LacCer, was involved in neutrophil apoptosis, which was mediated through Fas-dependent signal transduction.

Materials and Methods

Abs and other reagents

Mouse anti-PtdGlc IgM DIM21 and mouse anti-LacCer IgM T5A7 were prepared as described (5, 17, 19). Mouse anti-human Fas (CD95) IgM CH-11 and IgG ZB4 were obtained from Medical and Biological Laboratories (Nagoya, Japan). Mouse PE-conjugated anti-CD11b IgG ICRF44, PerCP–Cy5.5–anti-CD14 IgG 61D3, and PE-CD54 IgG HA58 were purchased from eBioscience (San Diego, CA). Mouse anti-Fas IgG DX2 and mouse anti-CD15s IgM CSLEX1 were from BD Biosciences (San Jose, CA). Complete protease inhibitor mixture (Complete) was obtained from Roche (Indianapolis, IN). PP1 was obtained from Biomol Research Laboratories (Plymouth Meeting, PA). LY294002, cysteine-containing aspartate-specific protease 3 (caspase-3) inhibitor VII, caspase-8 inhibitor II, caspase-9 inhibitor III, and superoxide dismutase ([SOD] from bovine erythrocytes) were obtained from Calbiochem (La Jolla, CA). Catalase (from bovine liver) was from Wako Pure Chemical Industries, (Osaka, Japan). fMLP and PMA were from Sigma-Aldrich (St. Louis, MO). All other reagents were of analytical grade.

Cell preparation and culture

Human neutrophils were isolated from heparinized peripheral blood of healthy volunteers, with their informed consent, using Polymorphprep (Nycomed Pharma, Oslo, Norway), centrifuged as described previously (6), and suspended at 10^7 cells/ml in DMEM/F12 medium. The neutrophil population was >95% pure, as determined by Wright–Giemsa staining, and viability was always >99%, as determined by trypan blue dye exclusion (Wako).

Monocyte-derived dendritic cells (DCs) were prepared from peripheral blood as described previously, with slight modifications (20). Briefly, mononuclear cells were isolated from peripheral human blood using Lymphoprep (Nycomed Pharma, Oslo, Norway), and monocytes were isolated from mononuclear cells using a monocyte isolation kit (Miltenyi Biotec, Bergisch Gladbach, Germany). DCs were differentiated from monocytes by incubation in RPMI 1640 medium supplemented with 10% autologous human serum, 100 U/ml GM-CSF (R&D Systems, Minneapolis, MN), and 50 ng/ml IL-4 (R&D Systems) in a CO_2 incubator for 3 d.

Liquid chromatography-tandem mass spectrometry analysis

Neutrophils were extracted twice with chloroform/methanol ([C/M] 2:1, v/v) and twice with chloroform/methanol/water (5:8:3, v/v/v) and then the extracts were dried under a stream of nitrogen gas. The dried extract was treated twice with propidium iodide (PI)-specific phospholipase C (Sigma-Aldrich). The resulting reaction mixture was lyophilized, and PtdGlc was further purified by HPLC (PU980; JASCO, Hachioji, Japan), using a Mono Bis normal- phase HPLC column (3.2Φ × 50 mm; Kyoto Monotech, Kyoto, Japan) equilibrated with C/M (8:2, v/v). The column was washed with C/M (8:2, v/v) for 2 min at a flow rate of 1 ml/min, and the bound materials were eluted with a gradient from C/M (8:2, v/v) to chloroform/methanol/water (7:3:0.3, v/v/v) for 4 min, followed by final solvent for 2 min. The column eluates were fractionated at 0.2 ml/tube and monitored with TLC. PtdGlc-containing fractions were collected, dried, and dissolved in 50 μl C/M (9:1, v/v). Aliquots of 2 μl were subjected to mass spectrometry (MS) analysis. MS was performed with a NanoFrontier L (Hitachi High-Technologies, Tokyo Japan), as described previously (21).

Flow cytometric analysis

The expression of cell-surface Ags was assessed by flow cytometry using a FACSCalibur (BD Biosciences), as described (5). Briefly, neutrophils were stained with Alexa Fluor 488–anti-PtdGlc IgM DIM21, Alexa Fluor 647–anti-LacCer IgM T5A7, or Alexa Fluor-labeled normal IgM for 30 min on ice. In some experiments, neutrophils were incubated with or without T5A7 or DIM21 at 37°C for 15 min, followed by staining with Alexa Fluor 488-conjugated DIM21 (Alexa Fluor 488-DIM21) or Alexa Fluor 647-conjugated T5A7 (Alexa Fluor 647-T5A7) on ice for 30 min, respectively. In some experiments, neutrophils were incubated at 37°C for 30 min before staining with Abs on ice for 30 min.

Immunostaining

Aliquots of 2 × 10^6 neutrophils were fixed with periodate-lysine paraformaldehyde (PLP) fixative solution (2% paraformaldehyde, 0.1 M lysine, and 0.2% sodium periodate in 50 mM phosphate buffer [pH 7.4]) for 30 min on ice. The cells were washed and blocked by incubation with 0.1% BSA and 5% normal goat serum in PBS for 60 min on ice. Aliquots of cells were permeabilized with 5 μg/ml digitonin for 10 min on ice and blocked with 0.1% BSA and 5% normal goat serum. The cells were stained with Alexa Fluor 546-DIM21 and Alexa Fluor 488-T5A7 for 30 min on ice. The stained cells were examined with a TCS-SP2 Leica confocal microscope equipped with a Plan-Apochromat 100× oil-immersion differential interference contrast (DIC) objective. Images were evaluated using multicolor/two-dimensional cytofluorogram software from Leica Microsystems. The software quantifies the extent of colocalization by creation of a binary mask of the image data in the cytofluorogram. The binary mask is created by masking all of the pixels that are double positive for Alexa Fluor 546-DIM21 and Alexa Fluor 488-T5A7 fluorescence. Colocalization was then assessed using the mask intensity rate for the colocalized Alexa Fluor 546 versus the overall intensities of the Alexa Fluor 546 in the image. A mask intensity rate >50% was used to confirm colocalization.

To assess the effects of anti-PtdGlc IgM DIM21 and anti-Fas IgG DX2 on the formation of PtdGlc and Fas clusters on the plasma membrane, neutrophils were incubated with or without 5 μg/ml anti-Fas IgG DX2, anti-PtdGlc IgM DIM21, or anti-sialyl Le^x IgM CSLEX1 at 37°C for 5 min, followed by additional incubation for 25 min on ice. As negative controls, neutrophils were incubated at 37°C for 5 min without Ab (–) and then incubated for an additional 25 min on ice with DIM21. The cells were washed three times with ice-cold PBS, fixed with PLP fixative solution for 30 min on ice, blocked with 0.1% BSA and 5% normal goat serum in PBS, incubated with DIM21 or DX2 for 30 min on ice, and then stained with fluorescein-conjugated secondary Abs.

Migration assay

Cell migration was assayed using a modified Boyden chamber with cellulose nitrate filters with a pore size of 3 μm (Sartorius, Göttingen, Germany), as described (8). Briefly, 0.1 μg/ml normal IgM, T5A7, or several concentrations of DIM21 in DMEM/F12 medium supplemented with 1 mg/ml BSA (DMEM/F12-BSA) were placed into the lower compartment of the chamber. Commercially available BSA has been reported to contain LPS as a contaminant (22). Several neutrophil functions, including superoxide generation and chemotaxis, can be modulated by 1–100 ng/ml LPS. The *Limulus* amebocyte lysate test using TOXICOLOR DIA-MP Set (Seikagaku Bioscience, Tokyo Japan) confirmed that BSA used in this study contained <10 pg/ml LPS, suggesting that contaminated LPS minimally affects neutrophil function. Aliquots of 300 μl cell suspensions (2.5 × 10^6 cells/ml) in DMEM/F12-BSA were placed into the upper compartment and incubated for 30 min at 37°C in a CO_2 incubator. The filters were fixed with neutral buffered formalin for 20 min and stained with Mayer's hematoxylin. The distance (μm) from the top of the filter to the furthest two cells in the same focal plane was measured microscopically with a 40× objective in 20 fields across the filter, and the results were expressed as the migration index (relative neutrophil migration:average distance of tested group/average distance of corresponding vehicle control). fMLP at a concentration of 10 nM was used in each assay as a positive reference chemoattractant.

Superoxide generation assay

Superoxide generation from neutrophils was assayed by measuring SOD-inhibited cytochrome *c* reduction, as described (5). Aliquots of 100 μl neutrophils (2.5 × 10^5 cells/100 μl) in DMEM/F12-BSA were incubated with or without 50 μg/ml SOD at 37°C for 30 min in 96-well plates, which had been precoated with DIM21, T5A7, or normal IgM, in a CO_2 incubator. As control experiments, neutrophils were incubated with 500 nM fMLP or 0.1% DMSO in BSA-coated wells at 37°C for 30 min. The

absorbance of the supernatants at 550 nm was measured with a Beckman DU640 spectrophotometer (Beckman Instruments, Fullerton, CA), and cytochrome *c* reduction was calculated using the formula: $E_{550} = 2.1 \times 10^4$ $M^{-1}cm^{-1}$ (23).

Annexin V-binding assay

Neutrophils (1×10^6 cells/ml) in DMEM/F12 medium supplemented with 10% FBS (DMEM/F12-FBS) were incubated with 4 or 8 μg/ml DIM21, T5A7, or normal IgM for 1 min, 1 h, and 4 h at 37°C in a CO_2 incubator. The apoptotic activity of DIM21 on neutrophils was sometimes changed by batch-to-batch variation. Moreover, the biological activity of DIM21 is not stable. Thus, the optimal working concentration of DIM21 was adjusted in each experiment. Usually, the submaximal concentration showing the maximum apoptotic activity of DIM21 was 8 μg/ml. In some experiments, neutrophils were preincubated for 30 min on ice with caspase-3 inhibitor VII (50 μM), caspase-8 inhibitor II (50 μM), caspase-9 inhibitor III (50 μM), PP1 (2 μM), or LY294002 (2 μM).

To determine the involvement of reactive oxygen species (ROS) in DIM21-induced neutrophil apoptosis, neutrophils were preincubated with 10 μM diphenyleneiodonium (DPI) for 30 min at 37°C in DMEM/F12-FBS (24). The loaded cells were then incubated with 4 μg/ml normal IgM or anti-PtdGlc DIM21 at 37°C for 4 h. To determine the effects of catalase on anti-PtdGlc Ab-induced apoptosis, neutrophils were incubated with DIM21 in the absence or presence of 140 U/ml SOD or 200 U/ml catalase at 37°C for 4 h. To determine the effects of anti-Fas Ab ZB4 on DIM21-induced neutrophil apoptosis, neutrophils (2.5×10^6 cells/ml) were preincubated with 10 μg/ml ZB4 for 1 h on ice prior to DIM21 treatment.

The binding of Alexa Fluor 488-conjugated Annexin V to cells was used as a sensitive method for measuring apoptosis (25). Specific binding of Annexin V was determined by Alexa Fluor 488-conjugated Annexin V and PI for Apoptosis Detection kit (Invitrogen), according to the manufacturer's instructions. The Annexin V-bound cells were analyzed using a FACSCalibur flow cytometer. The binding assay indicated that Annexin V did not bind to DIM21 (Supplemental Fig. 1).

TUNEL assay

The TUNEL assay with fluorescein-dUTP, using an In situ Cell Death Detection Kit (Roche Molecular Biochemicals, Indianapolis, IN), was used to detect and quantify DNA strand breaks in apoptotic neutrophils, according to the manufacturer's instructions. The stained cells were examined with a TCS-SP2 Leica confocal microscope equipped with a Plan-Apochromat 63× oil-immersion DIC objective.

Colorimetric measurement of caspase-3 activity

Neutrophils (2×10^6 cells/ml) were incubated with 1 μg/ml DIM21, normal IgM, or T5A7 in DMEM/F12-FBS at 37°C for 4 h in a CO_2 incubator. The caspase-3 activity of the cells was analyzed using an Apo-Alert caspase assay kit (Takara Bio, Shiga, Japan), according to the manufacturer's instructions.

Statistical analysis

The data are expressed as the means ± SD, and significant differences were analyzed by one-way ANOVA and post hoc test using the GraphPad PRISM statistical software package (GraphPad Software, San Diego, CA). In all analyses, $p < 0.05$ indicated statistical significance.

Results

PtdGlc is preferentially expressed on neutrophils

PtdGlc is a new type of glycolipid (16) that is preferentially expressed along the neutrophil-differentiation pathway (26). Consistent with these findings, we observed that PtdGlc was highly expressed on the cell surfaces of peripheral blood neutrophils ($CD14^{low}$ and $CD11b^{low}$) and weakly expressed on the cell surfaces of monocytes ($CD11b^{high}$ and $CD14^{high}$ cells) and lymphocytes ($CD54^+$ and $CD14^-$ cells; Fig. 1). Neutral glycosphingolipid LacCer has been identified as the neutrophil-differentiation marker CDw17 (27). Most cells highly expressing LacCer also showed high levels of PtdGlc expression (Fig. 1*B*). Peripheral blood-derived unstimulated DCs expressed LacCer, but did not express PtdGlc, on their cell surfaces (Fig. 1*A*). The presence of PtdGlc on neutrophils was also confirmed by liquid

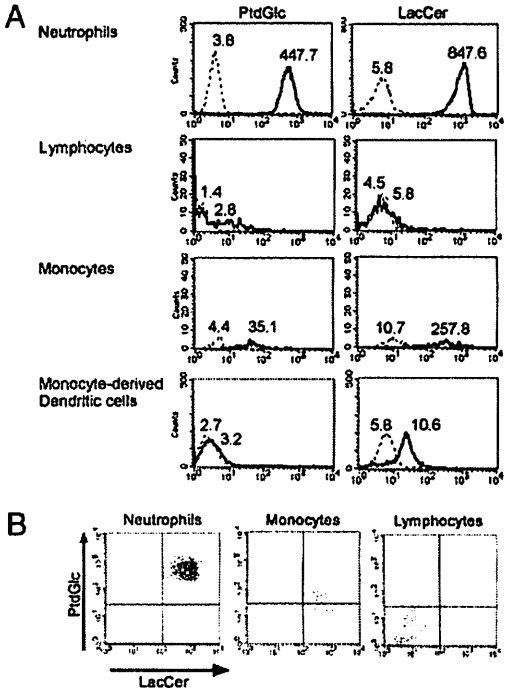

FIGURE 1. PtdGlc is a neutrophil marker in humans. *A*, Expression of PtdGlc on leukocytes. Peripheral blood samples were incubated with Alexa Fluor 488–anti-PtdGlc IgM DIM21, Alexa Fluor 647–anti-LacCer IgM T5A7, or Alexa Fluor-labeled normal IgM (dashed lines) for 30 min on ice. The erythrocytes were removed with erythrocyte-lysis buffer, and the remaining cells were analyzed by flow cytometry. Neutrophils ($CD14^{low}$ and $CD11b^{low}$), monocytes ($CD11b^{high}$ and $CD14^{high}$ cells), and lymphocytes ($CD54^+$ and $CD14^-$ cells) were gated using anti-CD11b, anti-CD14, and anti-CD54 mAbs. Monocyte-derived DCs were isolated as described in *Materials and Methods*. Numbers are the geometric means of fluorescence intensity. The results shown are representative data of four independent observations. *B*, Comparison of PtdGlc and LacCer expression on leukocytes. Leukocytes in *A* were stained with Alexa Fluor 488-DIM21 and Alexa Fluor 647-T5A7 on ice and analyzed by flow cytometry. The results shown are representative data of four independent observations.

chromatography/MS analyses (Fig. 2). PtdGlc was detected using a nano liquid chromatography-tandem mass spectrometry (LC/MS/MS) system after partial purification. Extracted ion current chromatogram by $m/z = 893.6$, which is the mass of a single molecular species of fetal murine brain PtdGlc, showed a peak at T12.6 (Fig. 2*A*). However, in the case of neutrophils, PtdGlc contained C18:0 fatty acyl chain as a major component. In addition, a peak with m/z of 935.6, identical to 6-*O*-acetylated, C18:0, 20:0-PtdGlc was also found at T10.3. A peak with m/z of 907.6 corresponding to 6-*O*-acetylated PtdGlc with C18:0, 18:0 was also found at T10.7, but the ratio relative to PtdGlc was less than that of C18:0, 20:0-PtdGlc. These molecular species were confirmed as PtdGlc-related compounds by MS and LC/MS/MS spectra (Fig. 2*B*). The fragmentation profile is comparable to previous results (28). LacCer was found to be the major glycolipid component of neutrophils, whereas PtdGlc content was ~0.75% of the lactosylceramide content estimated from the liquid chromatography/MS peak area.

PtdGlc forms domains that differ from LacCer-enriched microdomains

Human neutrophils abundantly express LacCer on their cell surfaces, and LacCer clusters to form lipid rafts coupled with Lyn on the plasma membranes of neutrophils and HL-60 cells (5). PtdGlc also forms raft-like membrane domains and activates Lyn in HL-

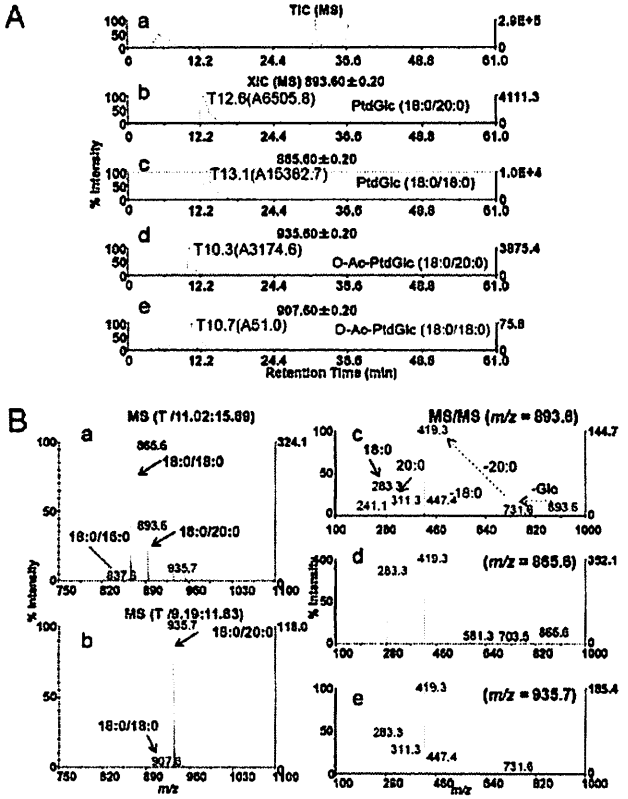

FIGURE 2. MS of PtdGlc in normal human neutrophils. *A*, MS chromatograms of PtdGlc. Total lipid extract from normal human neutrophils (10^8) was pretreated with PI-specific phospholipase C to remove PI. The major glycolipid, LacCer, was also separated from PtdGlc by HPLC equipped with a MonoBis normal phase column. The partially purified sample was then analyzed using a nano LC/MS/MS system. *a*, Total ion chromatogram; *b–e*, MS chromatogram scanned with m/z of 893.6 (*b*, PtdGlc with 18:0/20:0), 865.6 (*c*, PtdGlc with 18:0, 18:0), 935.6 (*d*, 6-*O*-Ac-PtdGlc with 18:0/20:0), and 907.6 (*e*, 6-*O*-Ac-PtdGlc with 18:0, 18:0). The results shown are representative data of two experiments. *B*, MS spectra (*a*, *b*) and LC/MS/MS spectra (*c–e*) of neutrophil PtdGlc-related molecules. PtdGlc (*a*) and 6-*O*-Ac-PtdGlc (*b*) production spectrum of PtdGlc with 18:0, 20:0 (*c*) and 18:0, 20:0 (*d*) and 6-*O*-Ac-PtdGlc with 18:0, 20:0 (*e*).

60 cells (16). Therefore, PtdGlc may be located in the LacCer-enriched lipid rafts and be involved in LacCer-mediated functions.

Pretreatment with anti-LacCer Ab T5A7 or anti-PtdGlc Ab DIM21 did not affect the binding of DIM21 or T5A7 to neutrophils, respectively (Fig. 3*A*), suggesting that these Abs do not recognize the same binding sites. Confocal fluorescence microscopy revealed that Alexa Fluor 488-DIM21$^+$ regions were not colocalized with Alexa Fluor 647-T5A7$^+$ regions on the plasma membrane or in granules of neutrophils (Fig. 3*B*). The mask intensity rates of the plasma membrane (6.5%) and whole cells (0.2%) were <50% (Fig. 3*C*, 3*D*). These observations suggested that PtdGlc and LacCer form different domains on the plasma membrane and are located in different granules of neutrophils.

The temperature-dependent spontaneous upregulation of surface $\alpha_M\beta_2$ integrin (CD11b/CD18) is an important characteristic of neutrophils (29). $\alpha_M\beta_2$ Integrin, which is expressed on the plasma membrane and is located in secretory vesicles and gelatinase granules, is translocated to the plasma membrane by incubation at 37°C (29, 30). More than 70% of LacCer is located in specific and azurophil granules (5) and is not translocated to the plasma membrane by incubation at 37°C for short periods (Fig. 3*E*). In contrast, PtdGlc was upregulated in a temperature-dependent manner. The upregulated expression of PtdGlc was not downregulated by cooling on ice (Supplemental Fig. 2). These observations suggested that, as in the case of $\alpha_M\beta_2$ integrin, PtdGlc exists in the granules, which are translocated to the plasma membrane in a temperature-dependent manner. Although anti-LacCer Ab T5A7 activates signal-transduction molecules, including Lyn and p38 MAPK, T5A7 did not enhance the expression of PtdGlc on the cell surface.

LacCer mediates neutrophil chemotaxis and the generation of superoxide (5, 6, 8). Anti-LacCer Ab T5A7 induced superoxide generation from neutrophilic-differentiated HL-60 cells with a bell-shaped dose-response curve from 0.01–10 μg/ml (8). Therefore, we also examined the effects of DIM21 on neutrophil chemotaxis and the generation of superoxide to determine whether PtdGlc is also involved in these LacCer-mediated activities. However, we found that DIM21 minimally enhanced migration (Fig. 3*F*) or superoxide generation (Fig. 3*G*), suggesting that PtdGlc is not involved in LacCer-mediated neutrophil functions.

PtdGlc is involved in neutrophil apoptosis

Neutrophils are short-lived cells that survive in the circulation for ~24–36 h before undergoing apoptosis (31). Therefore, neutrophil turnover is rapid, and the efficient removal of such large numbers of effete cells by apoptosis is a major homoeostatic endeavor (7). PtdGlc was already shown to be expressed on myelocytes, and anti-PtdGlc Ab was able to induce the differentiation of HL-60 cells to neutrophilic cells, suggesting that PtdGlc may be involved in differentiation-related events, including apoptosis, in neutrophils. Therefore, we first examined the effects of anti-PtdGlc IgM DIM21 on Annexin V expression in neutrophils to determine whether PtdGlc induces apoptosis of neutrophils, because Annexin V is a sensitive probe used to quantify the cells that undergo apoptosis (32). DIM21 treatment induced Annexin V$^+$ cells in an incubation time-dependent manner (Fig. 4). In contrast, anti-LacCer Ab did not enhance neutrophil apoptosis. Human monoclonal IgM GL-2, which specifically reacts with PtdGlc (13), and recombinant GL-2 Fab fragment rGL-7 also induced Annexin V$^+$ cells (Fig. 4*C*). PI positivity indicates necrotic cells. As shown in Fig. 4*A*, the percentages of PI$^+$ DIM21-treated cells (~6% of total after 4 h of incubation) were almost the same as those of other Ab-treated cells. Thus, DIM21 was unlikely to have induced necrosis of neutrophils.

The TUNEL reaction is also used to measure apoptosis, because DNA cleavage generally occurs at a much greater frequency in apoptotic cells than in nonapoptotic cells. Therefore, we tested the apoptotic effect of DIM21 on neutrophils by the TUNEL method. Neutrophils with typical apoptotic morphology, including rounding of nuclei, were observed after 4 h of incubation with DIM21, and these cells were TUNEL$^+$ (Fig. 5*A*). As shown in Fig. 5*C*, DIM21-induced TUNEL$^+$ cells were significantly increased by DIM21 treatment (26.8 ± 4.6%, mean ± SD of three experiments), but not by T5A7 treatment (19.0 ± 5.4), compared with those in normal IgM-treated cells (14.9 ± 5.6). Moreover, caspase-3 activation, which is another hallmark event leading to apoptosis (33), was significantly induced by treatment with DIM21 for 4 h but not by T5A7 (Fig. 5*D*). These observations suggested that PtdGlc mediates neutrophil apoptosis, whereas LacCer does not participate in this process.

PtdGlc-induced apoptosis is dependent on caspases but not Src family kinase, PIP_3 kinase, or superoxide generation

Despite the numerous available apoptotic stimuli, the final changes in the cells are similar, and many of the signaling events seem to

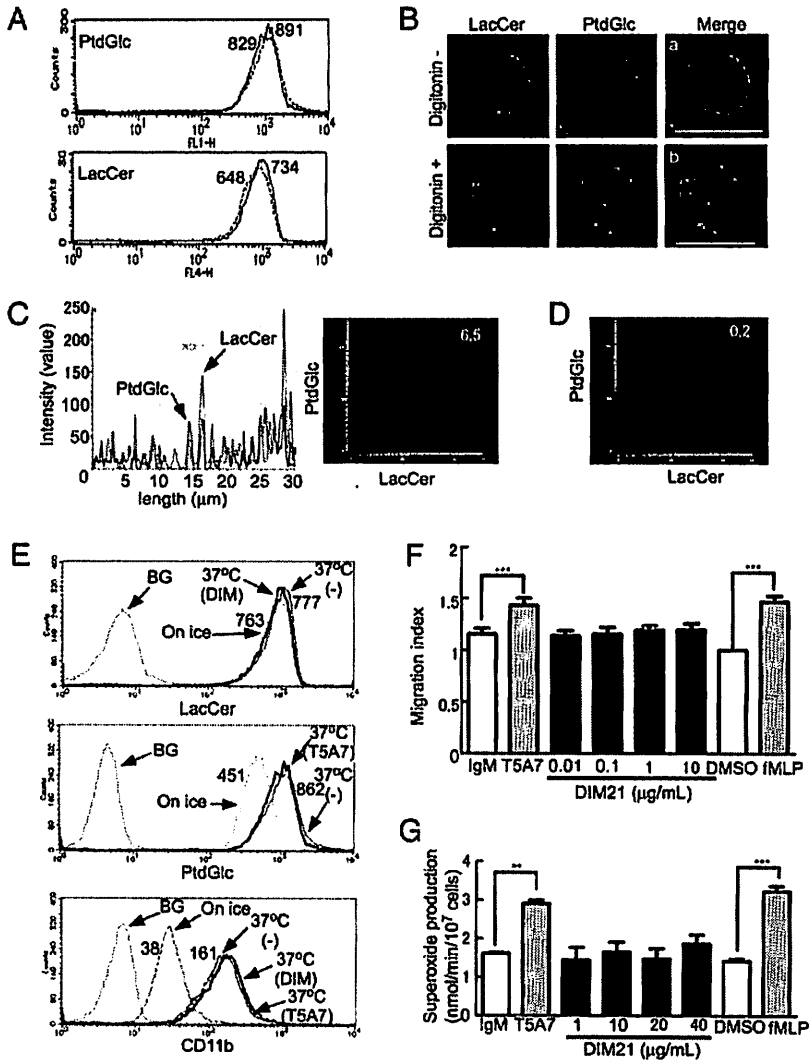

FIGURE 3. PtdGlc is present in different domains from LacCer-enriched lipid rafts. *A*, Effects of T5A7 on the expression of PtdGlc. Neutrophils were incubated with 1 μg/ml T5A7 or DIM21 on ice for 30 min, fixed, and stained with Alexa Fluor 488-DIM21 (PtdGlc) or Alexa Fluor 647-T5A7 (LacCer), respectively. Dashed lines indicate normal IgM-treated cells. Numbers represent the geometric means of fluorescence intensity. *B*, Colocalization of PtdGlc and LacCer on neutrophils. Neutrophils were fixed with PLP fixative solution for 30 min on ice and then treated (Digitonin +) or not (Digitonin −) with 5 μg/ml digitonin for 10 min. After washing, the cells were incubated with Alexa Fluor 488-conjugated anti-LacCer T5A7 IgM (green) and Alexa 546-conjugated anti-PtdGlc DIM21 IgM (red). The stained cells were examined with a TCS-SP2 Leica confocal microscope equipped with a Plan-Apochromat 100× oil-immersion DIC objective. Scale bar, 10 μm. The data shown are representative data of three experiments. *C*, Fluorescence intensity profiles of plasma membrane area in image overlays shown in *Ba* (*left panel*). *Right panel*, Cytofluorogram from Alexa Fluor 488-conjugated anti-LacCer T5A7 (LacCer) and Alexa Fluor 546-conjugated anti-PtdGlc DIM21 (PtdGlc) in image overlays shown in the *left panel*. The mask intensity rate was 6.5%. *D*, Cytofluorogram from Alexa Fluor 488-T5A7 (LacCer) and Alexa Fluor 546-anti-PtdGlc DIM21 (PtdGlc) in image overlays shown in *Bb*. The mask intensity rate was 0.2%. *E*, Temperature-dependent upregulation of PtdGlc. Neutrophils were incubated with or without (−) 1 μg/ml DIM21 (DIM) or T5A7 at 37°C for 15 min. Some cells were incubated without Abs on ice for 15 min (On ice). The cells were then stained with Alexa Fluor 647-T5A7 (*a*), Alexa Fluor 488-DIM21 (*b*), or PE-anti-CD11b (*c*) on ice for 30 min. The cells were washed, and the binding of each Ab to neutrophils was analyzed by flow cytometry. BG, Cells were treated with normal IgM on ice and stained with Alexa Fluor 647-, Alexa Fluor 488-, or PE-conjugated anti-IgM. Numbers are the geometric means of fluorescence intensity of neutrophils without Ab incubating on ice (On ice) or at 37°C [0.37°C (−)]. *F*, Effects of anti-PtdGlc Ab on neutrophil chemotaxis. Anti-PtdGlc Ab DIM21, anti-LacCer Ab T5A7, and normal IgM were assessed for chemotactic activities against neutrophils by the Boyden chamber method. IgM, 0.1 μg/ml normal IgM; T5A7, 0.1 μg/ml anti-LacCer Ab T5A7; DMSO, solvent control for fMLP stimulation; fMLP, 10 nM fMLP. Each bar shows the mean ± SD of four independent experiments. $***p < 0.001$. *G*, Effects of anti-PtdGlc Ab on neutrophil superoxide generation. The superoxide generation assay was performed as described in *Materials and Methods*. $**p < 0.01$, $***p < 0.001$. IgM, 10 μg/ml normal IgM; T5A7, 10 μg/ml anti-LacCer Ab T5A7; DMSO, solvent control for fMLP stimulation; fMLP, 500 nM fMLP. Each bar shows the mean ± SD of three independent experiments.

converge into common mechanisms involving activation of caspases (34). Death receptors, such as Fas, transmit death signals after stimulation by their specific ligands. Stimulation of death receptors leads to activation of the initiator caspase-8, which sequentially activates effector caspases, such as caspase-3, leading to apoptotic cell death (35). Caspase-3 is the final downstream effector caspase mediating apoptosis in neutrophils (36). Functional inhibitor studies suggested that caspase-9 is crucial for caspase-3 and -8 activation, at least in neutrophils (37). Therefore, we examined the involvement of these caspases in PtdGlc-mediated neutrophil apoptosis. As shown in Fig. 6*A*, specific inhibitors of caspases-3, -8, and -9 significantly inhibited DIM21-

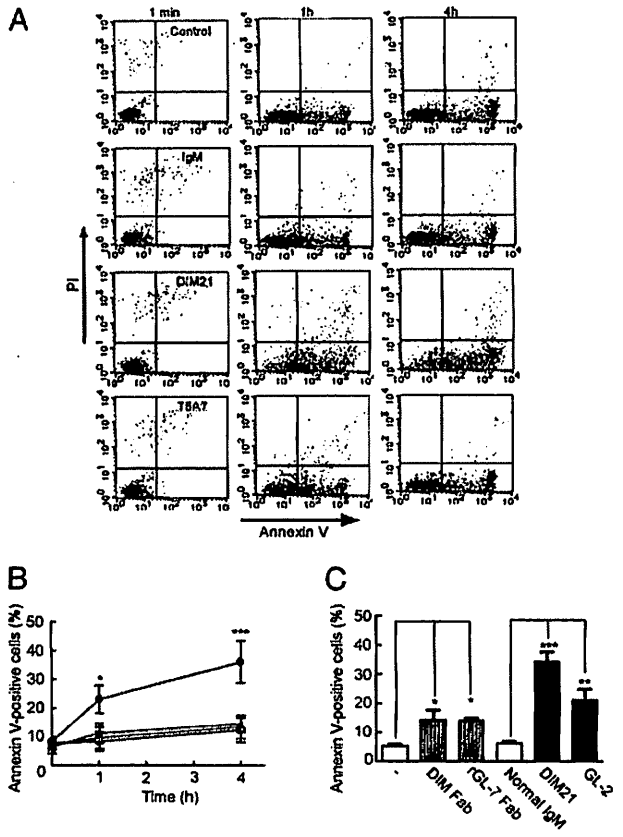

FIGURE 4. Effects of anti-PtdGlc Ab on neutrophil apoptosis. *A*, Neutrophils were incubated without (Control) or with 8 μg/ml anti-PtdGlc Ab DIM21, anti-LacCer Ab T5A7, or normal IgM at 37°C for 1 min, 1 h, and 4 h. The cells were then fixed and incubated with Alexa Fluor 488-conjugated Annexin V for 15 min at room temperature, stained with PI, and analyzed by flow cytometry. Representative results of three independent experiments are shown. *B*, Annexin V^+ and PI^- cells were gated as shown in *A*, and the numbers of Annexin V^+ cells were calculated. Each point represents the mean ± SD of three independent experiments. $*p < 0.05$, $***p < 0.001$. ●, DIM21; ○, without Ab; ▲, normal IgM; △, T5A7. *C*, Neutrophils were incubated without (−) or with 50 μg/ml Fab fragment of DIM21, 50 μg/ml recombinant Fab fragment of GL-2 (rGL-7), 8 μg/ml normal IgM; 8 μg/ml anti-PtdGlc Ab DIM21, or 2 μg/ml anti-PtdGlc human IgM GL-2 at 37°C for 4 h. The cells were then fixed and incubated with Alexa Fluor 488-conjugated Annexin V for 15 min at room temperature. Each bar shows the mean ± SD of three independent experiments. $*p < 0.05$, $**p < 0.01$, $***p < 0.001$.

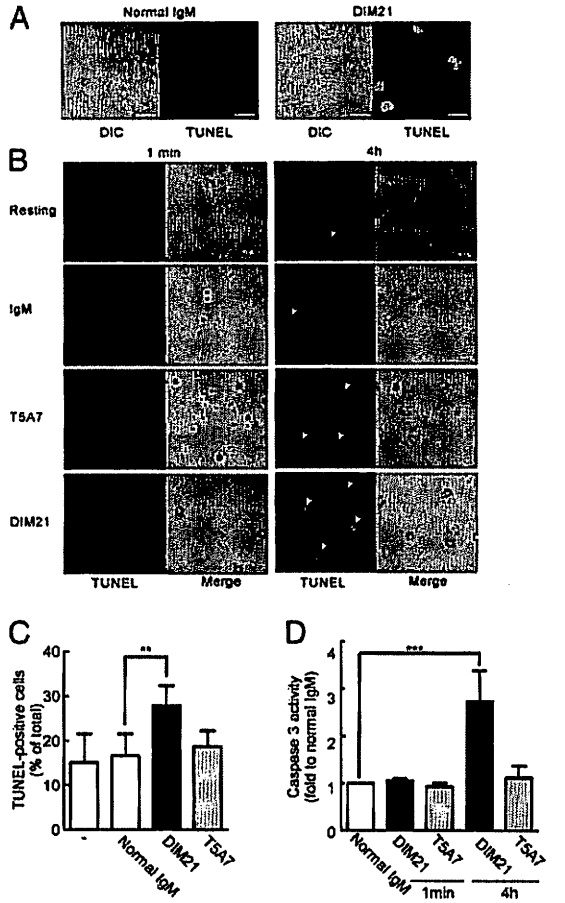

FIGURE 5. PtdGlc involvement in neutrophil apoptosis. *A*, Neutrophils were incubated with 8 μg/ml normal IgM or anti-PtdGlc Ab DIM21 at 37–C for 4 h. After incubation, cells were cytospun onto slide glasses and fixed with 4% paraformaldehyde, followed by staining with fluorescein-dUTP using an In situ Cell Death Detection Kit, as described in the *Materials and Methods*. Scale bars, 10 μm. *B*, Neutrophils were incubated with 8 μg/ml anti-PtdGlc Ab DIM21, anti-LacCer Ab T5A7, or normal IgM at 37°C for 1 min or 4 h. After incubation, cells were fixed with 4% paraformaldehyde. The cells with chromatin fragmentation were then stained with the chromatin fragmentation kit. The cells were examined with a TCS-SP2 Leica confocal microscope with a Plan-Apochromat 63× oil-immersion DIC objective. Scale bars, 10 μm. *C*, The $TUNEL^+$ cells, as shown in *B*, were counted. Data are shown as the means ± SD of three independent experiments. $**p < 0.01$. *D*, Effects of anti-PtdGlc Ab on caspase-3 activity. Neutrophils were incubated with 8 μg/ml anti-PtdGlc Ab DIM21, anti-LacCer Ab T5A7, or normal IgM at 37°C for 4 h, and caspase-3 activity of the cells was analyzed as described in *Materials and Methods*. Data are shown as the means ± SD of three independent experiments. $***p < 0.001$.

induced neutrophil apoptosis. Therefore, cross-linking of PtdGlc likely induces neutrophil apoptosis via the activation of caspases-8, -9, and -3.

In the case of LacCer-enriched lipid rafts, the activation of Src family kinases and PIP_3 kinases is thought to play crucial roles in LacCer-mediated signal transduction (1, 38). PtdGlc was demonstrated to form lipid raft-like domains and to be involved in rapid tyrosine phosphorylation of Src family protein kinases Lyn and Hck (16). Therefore, we examined the effects of the Src family kinase inhibitor PP1 and PIP_3 kinase inhibitor LY294002 on DIM21-induced neutrophil apoptosis. As shown in Fig. 6*B*, the Src family kinase inhibitor PP1 (2 μM) or the specific PIP_3 kinase inhibitor LY294002 (2 μM) did not affect DIM21-induced neutrophil apoptosis, whereas these concentrations completely inhibited LacCer-mediated neutrophil functions (6). Even a high concentration (10 μM) of PP1 or LY294002 and mixtures of these compounds did not affect DIM21-induced neutrophil apoptosis (data not shown). Lyn and PIP_3 kinase were shown to be involved in neutrophil survival (39, 40). Therefore, it is unlikely that Src family kinases, including Lyn, and PIP_3 kinases are involved in PtdGlc-mediated neutrophil apoptosis.

Several studies indicated that ROS are involved in neutrophil apoptosis (36, 41). The accumulation of ROS may initiate ceramide generation and the clustering of preformed Fas-inducing signaling complexes in lipid rafts (42). SOD enhances spontaneous neutrophil apoptosis, whereas catalase inhibits their spontaneous apoptosis and caspase-3 activation, suggesting that hydrogen peroxide is a potential mediator of ROS-induced neutrophil apoptosis in a caspase-dependent manner (43). Indeed, neutrophils from patients with chronic granulomatous disease, who

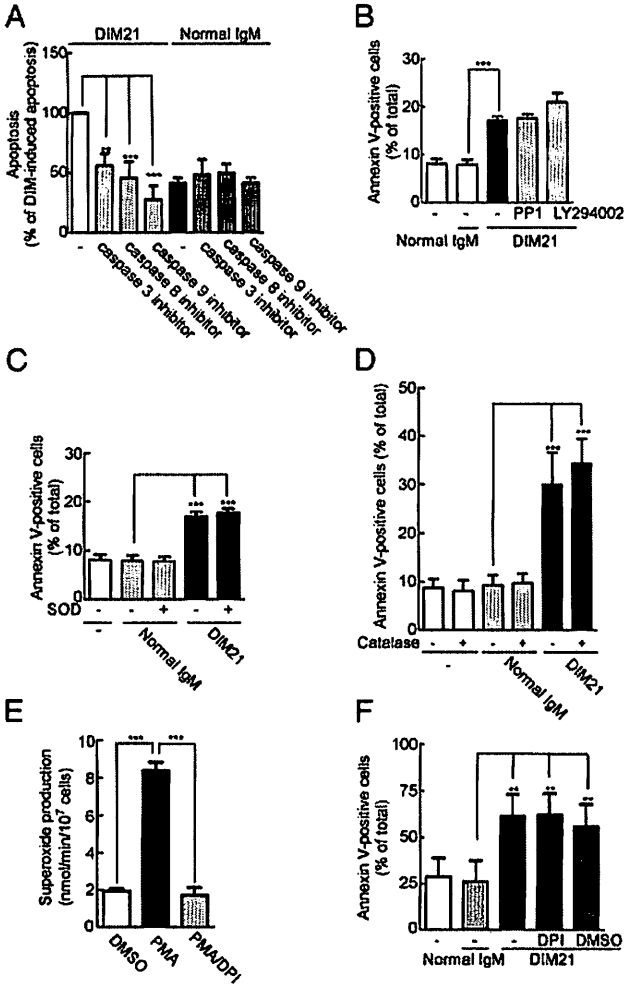

FIGURE 6. Effects of inhibitors of signal transduction molecules on PtdGlc-mediated apoptosis. *A*, Effects of caspase inhibitors on anti-PtdGlc Ab-induced apoptosis. Neutrophils were preincubated with 50 μM caspase-3 inhibitor VII, caspase-8 inhibitor II, or caspase-9 inhibitor III for 30 min on ice. The apoptosis ratio of each experiment was calculated as (percentage of DIM21- or normal IgM-induced apoptotic cells in the inhibitor-treated cells)/(percentage of DIM21-induced apoptotic cells). Each bar shows the mean ± SD of three independent experiments. *B*, Anti-PtdGlc Ab-induced apoptosis was not mediated by Src family kinases or PIP_3 kinases. Neutrophils were incubated with DMSO (as solvent control; −) 2 μM PP1, or LY294002 for 30 min on ice. These cells were incubated without (−) or with 1 μg/ml normal IgM or anti-PtdGlc DIM21 for 4 h at 37°C, and specific binding of Alexa Fluor 488-conjugated Annexin V to neutrophils was analyzed by flow cytometry. Each bar shows the mean ± SD of three independent experiments. *C*, Effects of SOD on anti-PtdGlc Ab-induced apoptosis. Neutrophils were incubated without (−) or with 4 μg/ml normal IgM or anti-PtdGlc Ab DIM21 in the absence (SOD −) or presence (SOD +) of 140 U/ml of SOD at 37°C for 4 h. Specific binding of Alexa Fluor 488-conjugated Annexin V to neutrophils was analyzed by flow cytometry. Representative results of three independent experiments are shown. The numbers in each panel are the percentages of Annexin V^+ cells. Each bar shows the mean ± SD of three independent experiments. *D*, Effects of catalase on anti-PtdGlc Ab-induced apoptosis. Neutrophils were incubated without (−) or with 4 μg/ml normal IgM or anti-PtdGlc DIM21 in the absence (catalase −) or presence (catalase +) of 200 U/ml catalase at 37°C for 4 h. Specific binding of Alexa Fluor 488-conjugated Annexin V to neutrophils was analyzed by flow cytometry. Representative results of three independent experiments are shown. The numbers in each panel are the percentages of Annexin V^+ cells. Each bar shows the mean ± SD of three independent experiments. *E*, Effects of DPI on PMA-induced neutrophil superoxide generation. Neutrophils were treated or not with 10 μM DPI for 30 min at 37°C. The loaded cells were then incubated with 10 nM PMA for 30 min at 37°C. Each bar shows the mean ± SD of three independent experiments. DMSO, solvent control for PMA stimulation. *F*, Effects of DPI on anti-PtdGlc Ab-induced neutrophil apoptosis. Neutrophils were treated or not with 10 μM DPI for 30 min at 37°C. The loaded cells were then incubated with 4 μg/ml anti-PtdGlc Ab DIM21 for 4 h at 37°C. Each bar shows the mean ± SD of three independent experiments. $^{**}p < 0.01$, $^{***}p < 0.001$.

have a deficiency in NADPH oxidase activity, also undergo spontaneous apoptosis but have a prolonged lifespan (44). However, another group could not detect a difference in the rate of spontaneous apoptosis between normal and NADPH oxidase-deficient neutrophils (7). Neither SOD nor catalase affected DIM21-induced neutrophil apoptosis under our experimental conditions (Fig. 6*C*, 6*D*). DPI, which is a strong NADPH oxidase inhibitor, did not inhibit DIM21-induced apoptosis, although it completely inhibited PMA-induced superoxide generation from neutrophils (Fig. 6*E*, 6*F*). DIM21 did not induce superoxide generation by itself (Fig. 3*G*). These observations suggested that it is unlikely that NADPH oxidase-mediated ROS is involved in PtdGlc-mediated neutrophil apoptosis.

Fas is involved in PtdGlc-mediated apoptosis

Fas is a death receptor associated with lipid rafts during Fas-mediated apoptosis (45–47). Therefore, we examined whether PtdGlc is colocalized with Fas in neutrophils. PtdGlc and Fas were colocalized on the plasma membranes in resting neutrophils. PtdGlc formed large clusters and was colocalized with Fas following stimulation with anti-PtdGlc IgM DIM21 (Fig. 7*A*). Moreover, treatment with anti-Fas IgG DX2, which can induce apoptosis, caused the formation of Fas clusters, which were also colocalized with PtdGlc (Fig. 7*B*). The mask intensity rates of resting, DIM21-treated, or DX2-treated neutrophils were 85.7, 89.5, and 90.4%, respectively (Fig. 7*C*). Neutrophils also expressed high levels of CD15s (sialyl Le^x Ag) on their cell surfaces. However, treatment with anti-CD15s IgM did not induce Fas-colocalized cluster formation. The mask intensity rate of anti-CD15s IgM-treated neutrophils was only 1.7%. These observations suggested that PtdGlc forms large clusters with Fas along with activating cells through the cross-linking of PtdGlc or Fas. Fas is activated by inducing its trimerization (48). Activated Fas recruits adaptor molecules, such as FADD, which recruit procaspase-8 to the receptor complex where it undergoes autocatalytic activation. Incubation of neutrophils with agonistic anti-Fas Abs significantly accelerates the apoptotic process in these cells (25, 49). The Fas agonistic Ab CH-11 was presumed to mediate its apoptotic effect through cross-linking of Fas receptors, in a manner analogous to the Fas ligand. In contrast, the Fas antagonistic Ab ZB4 can effectively block apoptosis induced by CH-11 by binding to the same epitope as CH-11 (50). ZB4 inhibits Fas ligation and efficiently blocks apoptotic cell death induced by the agonistic anti-Fas IgM CH-11 or Fas ligand in human neutrophils (51). We found that ZB4 significantly inhibited CH-11– and DIM21-induced neutrophil apoptosis (Fig. 7*E*). Therefore, the Fas-mediated activation of FADD seems to be involved in PtdGlc-mediated neutrophil apoptosis.

Discussion

More than 400 species of glycolipid have been identified based on the sugar chain structures (52). Glycolipids have attracted considerable interest because leukocytes show lineage-related and differentiation-dependent expression of these molecules, making

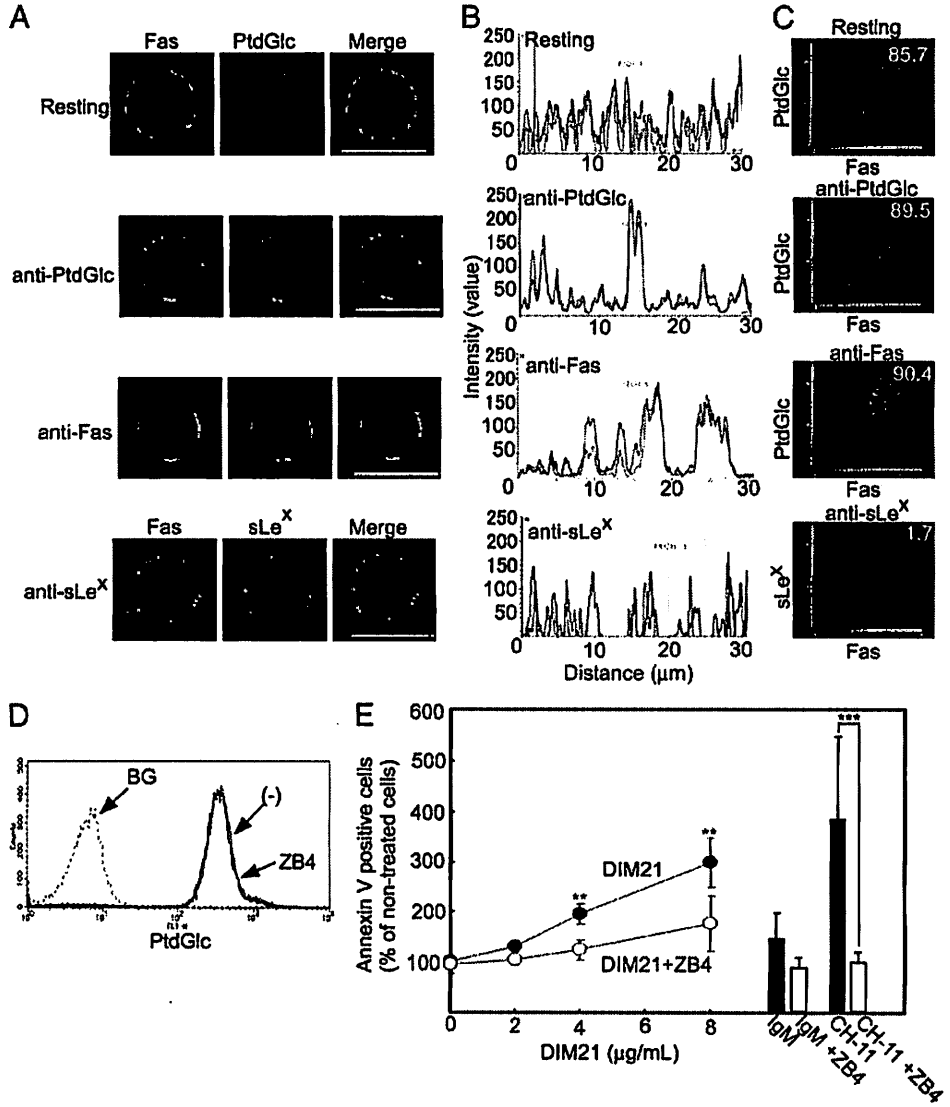

FIGURE 7. Association of PtdGlc and Fas. *A*, Colocalization of Fas and PtdGlc. Neutrophils (2×10^6 cells/ml) were incubated without (Resting) or with 5 μg/ml anti-Fas IgGDX2, anti-PtdGlc IgM DIM21, or anti-sialyl Le^x IgM CSLEX1 at 37°C for 5 min. The cells were washed with 10 volumes of ice-cold PBS, fixed with PLP, and treated sequentially with primary DX2 or DIM21 Abs and secondary (Alexa Fluor 488-conjugated goat anti-mouse IgG or Alexa Fluor 647-conjugated rabbit anti-mouse IgM) Abs for 30 min on ice. The stained cells were examined with a TCS-SP2 Leica confocal microscope equipped with a Plan-Apochromat 100× oil-immersion DIC objective. Scale bars, 10 μm. *B*, Fluorescence intensity profiles of plasma membrane area in image overlays shown in *A*. *C*, Cytofluorogram from Alexa Fluor 488-conjugated anti-Fas IgG (Fas) and Alexa Fluor 546-conjugated anti-PtdGlc DIM21 (PtdGlc) in image overlays shown in *A*. The numbers indicate the mask intensity rates. *D*, Neutrophils were treated without (−) or with 10 μg/ml anti-Fas IgG ZB4 for 30 min on ice. After incubation, cells were washed and stained with Alexa Fluor 488-DIM21. BG, Cells were treated with normal IgM on ice and stained with Alexa Fluor 488-labeled anti-IgM. *E*, Effects of the Fas antagonist Ab ZB4 on PtdGlc-mediated neutrophil apoptosis. Neutrophils (2.5×10^6 cells/ml) were incubated or not without 10 μg/ml anti-Fas IgG ZB4 on ice for 60 min, followed by the addition of 2, 4, or 8 μg/ml anti-PtdGlc IgM DIM21, 4 μg/ml anti-Fas IgM CH-11(CH-11), or 4 μg/ml normal IgM and incubation at 37°C for 4 h. The binding of Annexin V to the cells was analyzed as described in *Materials and Methods*. ●, DIM21; ○, DIM21+ZB4. $^{**}p < 0.01$, $^{***}p < 0.001$.

them useful as differentiation markers. Although several types of glycolipid are present on neutrophils (53), the functions of most of these molecules, with the exception of LacCer, have not been well characterized. LacCer is a differentiation marker for human neutrophils (54, 55), but it is also expressed on monocytes (54) and monocyte-derived DCs (Fig. 1). In contrast, PtdGlc was weakly expressed on monocytes and lymphocytes, and it was not expressed on monocyte-derived DCs. Therefore, it is likely that PtdGlc, rather than LacCer, can be used as a highly specific differentiation marker for neutrophils.

Previous studies demonstrated the presence of heterogeneous lipid domains on plasma membranes in the same cells (56, 57). PtdGlc forms distinct lipid domains from glycosphingolipids on the outer leaflet of the plasma membrane of HL60 cells and the human alveolar epithelial cell line A549 (18). Confocal microscopic examination of neutrophils revealed that PtdGlc was not colocalized with LacCer on the plasma membrane of neutrophils (Fig. 3). LacCer mediates neutrophil chemotaxis and superoxide generation but not apoptosis (5, 8). In contrast, PtdGlc mediates neutrophil apoptosis but not chemotaxis or superoxide generation (Figs. 3, 4). LacCer-mediated signal transduction is highly dependent on the activation of Lyn and PIP_3 kinase (6, 58), whereas PtdGlc-mediated neutrophil apoptosis did not depend on Src family kinases or PIP_3 kinase (Fig. 6). Several studies demon-

strated that Src family kinases, including Lyn, suppress apoptosis by inhibiting caspase-8 activity (34). Many factors that promote neutrophil survival activate PIP_3 kinase (59). Therefore, it seems that LacCer and PtdGlc form different domains on the neutrophil plasma membrane and mediate different functions via different molecular mechanisms.

Apoptosis can be initiated by two main pathways: the death receptor-mediated pathway and the intrinsic mitochondrial pathway (60). The Fas-mediated pathway belongs to the death receptor pathway. Ligation of Fas induces the formation of a death-inducing signaling complex consisting of Fas, an adaptor protein (FADD) for Fas, and procaspase-8 (60). Fas and its ligand exist as trimers, and the clustering of Fas-containing domains following ligation is required to promote aggregation of procaspase-8 molecules within the death-inducing signaling complex (48). The coalescence of Fas-containing lipid rafts after ligation of this receptor is the initial step of Fas-induced apoptosis (61). Consistent with these results, we observed that cross-linking of Fas caused the formation of a large cluster of Fas-containing domains, which contained PtdGlc molecules (Fig. 7). Importantly, the cross-linking of PtdGlc also formed Fas-containing large clusters on the plasma membrane of neutrophils. Moreover, the Fas antagonistic Ab ZB4 significantly blocks apoptosis induced by CH-11 through binding to the same epitope as CH-11 (50). In contrast, the antagonistic anti-Fas IgG ZB4, which has the ability to prevent Fas ligation (51), significantly inhibited PtdGlc-mediated neutrophil apoptosis (Fig. 7*E*). Therefore, it is likely that the Fas-mediated pathway is responsible for PtdGlc-mediated neutrophil apoptosis.

Identification of the natural ligands for PtdGlc in vivo is the most important issue involving PtdGlc-mediated neutrophil apoptosis that remains to be resolved. PtdGlc-enriched raft-like domains express glucose clusters on the neutrophil plasma membrane. Glucose residues can be recognized by certain kinds of glucose-binding lectin, such as glucose/mannose-specific lectins and C-type animal lectins. Indeed, macrophage mannose receptors, which are expressed on human macrophages and lymphocytes, are capable of binding to glucose residues (62, 63). Apoptosis is the final step in the differentiation of neutrophils. Apoptosis is necessary to maintain a certain number of neutrophils in vivo and for macrophages to remove neutrophils from inflamed tissues, steps critical in limiting inflammatory tissue injury and the subsequent resolution of inflammation (2–4, 64). Apoptosis of neutrophils may be initiated by the binding of PtdGlc to natural ligands. Further studies are required to elucidate the biological significance of PtdGlc in neutrophils.

Disclosures

The authors have no financial conflicts of interest.

References

1. Yoshizaki, F., H. Nakayama, C. Iwahara, K. Takamori, H. Ogawa, and K. Iwabuchi. 2008. Role of glycosphingolipid-enriched microdomains in innate immunity: microdomain-dependent phagocytic cell functions. *Biochim. Biophys. Acta* 1780: 383–392.
2. Haslett, C. 1992. Resolution of acute inflammation and the role of apoptosis in the tissue fate of granulocytes. *Clin. Sci.* 83: 639–648.
3. Pitrak, D. L., H. C. Tsai, K. M. Mullane, S. H. Sutton, and P. Stevens. 1996. Accelerated neutrophil apoptosis in the acquired immunodeficiency syndrome. *J. Clin. Invest.* 98: 2714–2719.
4. Savill, J. S., A. H. Wyllie, J. E. Henson, M. J. Walport, P. M. Henson, and C. Haslett. 1989. Macrophage phagocytosis of aging neutrophils in inflammation. Programmed cell death in the neutrophil leads to its recognition by macrophages. *J. Clin. Invest.* 83: 865–875.
5. Iwabuchi, K., and I. Nagaoka. 2002. Lactosylceramide-enriched glycosphingolipid signaling domain mediates superoxide generation from human neutrophils. *Blood* 100: 1454–1464.
6. Nakayama, H., F. Yoshizaki, A. Prinetti, S. Sonnino, L. Mauri, K. Takamori, H. Ogawa, and K. Iwabuchi. 2008. Lyn-coupled LacCer-enriched lipid rafts are required for CD11b/CD18-mediated neutrophil phagocytosis of nonopsonized microorganisms. *J. Leukoc. Biol.* 83: 728–741.
7. Remijsen, Q., T. Vanden Berghe, E. Parthoens, B. Asselbergh, P. Vandenabeele, and J. Willems. 2009. Inhibition of spontaneous neutrophil apoptosis by parabutoporin acts independently of NADPH oxidase inhibition but by lipid raft-dependent stimulation of Akt. *J. Leukoc. Biol.* 85: 497–507.
8. Sato, T., K. Iwabuchi, I. Nagaoka, Y. Adachi, N. Ohno, H. Tamura, K. Seyama, Y. Fukuchi, H. Nakayama, F. Yoshizaki, et al. 2006. Induction of human neutrophil chemotaxis by *Candida albicans*-derived beta-1,6-long glycoside side-chain-branched beta-glucan. *J. Leukoc. Biol.* 80: 204–211.
9. Lingwood, D., H. J. Kaiser, I. Levental, and K. Simons. 2009. Lipid rafts as functional heterogeneity in cell membranes. *Biochem. Soc. Trans.* 37: 955–960.
10. Kniep, B., and K. M. Skubitz. 1998. Subcellular localization of glycosphingolipids in human neutrophils. *J. Leukoc. Biol.* 63: 83–88.
11. Spychalska, J., G. Smolcńska-Sym, E. Zdebska, J. Woźniak, and J. Kościelak. 2003. Quantitative analysis of LacCer/CDw17 in human myelogenous leukaemic cells. *Cell. Mol. Biol. Lett.* 8: 911–917.
12. Zimmerman, J. W., J. Lindermuth, P. A. Fish, G. P. Palace, T. T. Stevenson, and D. E. DeMong. 1998. A novel carbohydrate-glycosphingolipid interaction between a beta-(1-3)-glucan immunomodulator, PGG-glucan, and lactosylceramide of human leukocytes. *J. Biol. Chem.* 273: 22014–22020.
13. Nagatsuka, Y., T. Kasama, Y. Ohashi, J. Uzawa, Y. Ono, K. Shimizu, and Y. Hirabayashi. 2001. A new phosphoglycerolipid, 'phosphatidylglucose', found in human cord red cells by multi-reactive monoclonal anti-i cold agglutinin, mAb GL-1/GL-2. *FEBS Lett.* 497: 141–147.
14. Kawano-Yamamoto, C., K. Muroi, Y. Nagatsuka, M. Higuchi, S. Kikuchi, T. Nagai, S. I. Hakomori, and K. Ozawa. 2006. Establishment and characterization of a new erythroblastic leukemia cell line, EEB: phosphatidylglucoside-mediated erythroid differentiation and apoptosis. *Leuk. Res.* 30: 829–839.
15. Kinoshita, M. O., S. Furuya, S. Ito, Y. Shinoda, Y. Yamazaki, P. Greimel, Y. Ito, T. Hashikawa, T. Machida, Y. Nagatsuka, and Y. Hirabayashi. 2009. Lipid rafts enriched in phosphatidylglucoside direct astroglial differentiation by regulating tyrosine kinase activity of epidermal growth factor receptors. *Biochem. J.* 419: 565–575.
16. Nagatsuka, Y., M. Hara-Yokoyama, T. Kasama, M. Takekoshi, F. Maeda, S. Ihara, S. Fujiwara, E. Ohshima, K. Ishii, T. Kobayashi, et al. 2003. Carbohydrate-dependent signaling from the phosphatidylglucoside-based microdomain induces granulocytic differentiation of HL60 cells. *Proc. Natl. Acad. Sci. USA* 100: 7454–7459.
17. Nagatsuka, Y., Y. Horibata, Y. Yamazaki, M. Kinoshita, Y. Shinoda, T. Hashikawa, H. Koshino, T. Nakamura, and Y. Hirabayashi. 2006. Phosphatidylglucoside exists as a single molecular species with saturated fatty acyl chains in developing astroglial membranes. *Biochemistry* 45: 8742–8750.
18. Murate, M., T. Hayakawa, K. Ishii, H. Inadome, P. Greimel, M. Watanabe, Y. Nagatsuka, K. Ito, Y. Ito, H. Takahashi, et al. 2010. Phosphatidylglucoside forms specific lipid domains on the outer leaflet of the plasma membrane. *Biochemistry* 49: 4732–4739.
19. Yamazaki, Y., Y. Nagatsuka, E. Oshima, Y. Suzuki, Y. Hirabayashi, and T. Hashikawa. 2006. Comprehensive analysis of monoclonal antibodies against detergent-insoluble membrane/lipid rafts of HL60 cells. *J. Immunol. Methods* 311: 106–116.
20. Castelli, J., E. K. Thomas, M. Gilliet, Y. J. Liu, and J. A. Levy. 2004. Mature dendritic cells can enhance CD8+ cell noncytotoxic anti-HIV responses: the role of IL-15. *Blood* 103: 2699–2704.
21. Ito, S., T. Nabetani, Y. Shinoda, Y. Nagatsuka, and Y. Hirabayashi. 2008. Quantitative analysis of a novel glucosylated phospholipid by liquid chromatography-mass spectrometry. *Anal. Biochem.* 376: 252–257.
22. Haslett, C., L. A. Guthrie, M. M. Kopaniak, R. B. Johnston, Jr., and P. M. Henson. 1985. Modulation of multiple neutrophil functions by preparative methods or trace concentrations of bacterial lipopolysaccharide. *Am. J. Pathol.* 119: 101–110.
23. Someya, A., I. Nagaoka, K. Iwabuchi, and T. Yamashita. 1991. Comparison of O2(−)-producing activity of guinea-pig eosinophils and neutrophils in a cell-free system. *Comp. Biochem. Physiol. B* 100: 25–30.
24. Ellis, J. A., S. J. Mayer, and O. T. Jones. 1988. The effect of the NADPH oxidase inhibitor diphenyleneiodonium on aerobic and anaerobic microbicidal activities of human neutrophils. *Biochem. J.* 251: 887–891.
25. Liles, W. C., P. A. Kiener, J. A. Ledbetter, A. Aruffo, and S. J. Klebanoff. 1996. Differential expression of Fas (CD95) and Fas ligand on normal human phagocytes: implications for the regulation of apoptosis in neutrophils. *J. Exp. Med.* 184: 429–440.
26. Oka, S., Y. Nagatsuka, J. Kikuchi, T. Yokote, Y. Hirabayashi, T. Hanafusa, K. Ozawa, and K. Muroi. 2009. Preferential expression of phosphatidylglucoside along neutrophil differentiation pathway. *Leuk. Lymphoma* 50: 1190–1197.
27. Symington, F. W., D. L. Hedges, and S. Hakomori. 1985. Glycolipid antigens of human polymorphonuclear neutrophils and the inducible HL-60 myeloid leukemia line. *J. Immunol.* 134: 2498–2506.
28. Nagatsuka, Y., H. Tojo, and Y. Hirabayashi. 2006. Identification and analysis of novel glycolipids in vertebrate brains by HPLC/mass spectrometry. *Methods Enzymol.* 417: 155–167.
29. Graves, V., T. Gahig, L. McCarthy, E. F. Strour, T. Leemhuis, and D. English. 1992. Simultaneous mobilization of Mac-1 (CD11b/CD18) and formyl peptide chemoattractant receptors in human neutrophils. *Blood* 80: 776–787.
30. Sengeløv, H., L. Kjeldsen, M. S. Diamond, T. A. Springer, and N. Borregaard. 1993. Subcellular localization and dynamics of Mac-1 (alpha m beta 2) in human neutrophils. *J. Clin. Invest.* 92: 1467–1476.

31. Fadeel, B., A. Ahlin, J. I. Henter, S. Orrenius, and M. B. Hampton. 1998. Involvement of caspases in neutrophil apoptosis: regulation by reactive oxygen species. *Blood* 92: 4808–4818.
32. van Engeland, M., L. J. Nieland, F. C. Ramaekers, B. Schutte, and C. P. Reutelingsperger. 1998. Annexin V-affinity assay: a review on an apoptosis detection system based on phosphatidylserine exposure. *Cytometry* 31: 1–9.
33. Maianski, N. A., A. N. Maianski, T. W. Kuijpers, and D. Roos. 2004. Apoptosis of neutrophils. *Acta Haematol.* 111: 56–66.
34. Kurokawa, M., and S. Kornbluth. 2009. Caspases and kinases in a death grip. *Cell* 138: 838–854.
35. Guicciardi, M. E., and G. J. Gores. 2009. Life and death by death receptors. *FASEB J.* 23: 1625–1637.
36. Scheel-Toellner, D., K. Q. Wang, P. R. Webb, S. H. Wong, R. Craddock, L. K. Assi, M. Salmon, and J. M. Lord. 2004. Early events in spontaneous neutrophil apoptosis. *Biochem. Soc. Trans.* 32: 461–464.
37. Daigle, I., and H. U. Simon. 2001. Critical role for caspases 3 and 8 in neutrophil but not eosinophil apoptosis. *Int. Arch. Allergy Immunol.* 126: 147–156.
38. Suzuki, K. G., T. K. Fujiwara, F. Sanematsu, R. Iino, M. Edidin, and A. Kusumi. 2007. GPI-anchored receptor clusters transiently recruit Lyn and G alpha for temporary cluster immobilization and Lyn activation: single-molecule tracking study 1. *J. Cell Biol.* 177: 717–730.
39. Wang, K., D. Scheel-Toellner, S. H. Wong, R. Craddock, J. Caamano, A. N. Akbar, M. Salmon, and J. M. Lord. 2003. Inhibition of neutrophil apoptosis by type I IFN depends on cross-talk between phosphoinositol 3-kinase, protein kinase C-delta, and NF-kappa B signaling pathways. *J. Immunol.* 171: 1035–1041.
40. Wei, S., J. H. Liu, P. K. Epling-Burnette, A. M. Gamero, D. Ussery, E. W. Pearson, M. E. Elkahani, J. I. Diaz, and J. Y. Djeu. 1996. Critical role of Lyn kinase in inhibition of neutrophil apoptosis by granulocyte-macrophage colony-stimulating factor. *J. Immunol.* 157: 5155–5162.
41. Watson, R. W. 2002. Redox regulation of neutrophil apoptosis. *Antioxid. Redox Signal.* 4: 97–104.
42. Scheel-Toellner, D., K. Wang, R. Craddock, P. R. Webb, H. M. McGettrick, L. K. Assi, N. Parkes, L. E. Clough, E. Gulbins, M. Salmon, and J. M. Lord. 2004. Reactive oxygen species limit neutrophil life span by activating death receptor signaling. *Blood* 104: 2557–2564.
43. Yasui, K., N. Kobayashi, T. Yamazaki, K. Agematsu, S. Matsuzaki, S. Ito, S. Nakata, A. Baba, and K. Koike. 2005. Superoxide dismutase (SOD) as a potential inhibitory mediator of inflammation via neutrophil apoptosis. *Free Radic. Res.* 39: 755–762.
44. Kasahara, Y., K. Iwai, A. Yachie, K. Ohta, A. Konno, H. Seki, T. Miyawaki, and N. Taniguchi. 1997. Involvement of reactive oxygen intermediates in spontaneous and CD95 (Fas/APO-1)-mediated apoptosis of neutrophils. *Blood* 89: 1748–1753.
45. Gajate, C., and F. Mollinedo. 2001. The antitumor ether lipid ET-18-OCH(3) induces apoptosis through translocation and capping of Fas/CD95 into membrane rafts in human leukemic cells. *Blood* 98: 3860–3863.
46. Scheel-Toellner, D., K. Wang, R. Singh, S. Majeed, K. Raza, S. J. Curnow, M. Salmon, and J. M. Lord. 2002. The death-inducing signalling complex is recruited to lipid rafts in Fas-induced apoptosis. *Biochem. Biophys. Res. Commun.* 297: 876–879.
47. Legembre, P., S. Daburon, P. Moreau, J. F. Moreau, and J. L. Taupin. 2006. Modulation of Fas-mediated apoptosis by lipid rafts in T lymphocytes. *J. Immunol.* 176: 716–720.
48. Nagata, S. 1996. Fas-induced apoptosis, and diseases caused by its abnormality. *Genes Cells* 1: 873–879.
49. Iwai, K., T. Miyawaki, T. Takizawa, A. Konno, K. Ohta, A. Yachie, H. Seki, and N. Taniguchi. 1994. Differential expression of bcl-2 and susceptibility to anti-Fas-mediated cell death in peripheral blood lymphocytes, monocytes, and neutrophils. *Blood* 84: 1201–1208.
50. Fadeel, B., C. J. Thorpe, S. Yonehara, and F. Chiodi. 1997. Anti-Fas IgG1 antibodies recognizing the same epitope of Fas/APO-1 mediate different biological effects in vitro. *Int. Immunol.* 9: 201–209.
51. Tortorella, C., G. Piazzolla, F. Spaccavento, S. Pece, E. Jirillo, and S. Antonaci. 1998. Spontaneous and Fas-induced apoptotic cell death in aged neutrophils. *J. Clin. Immunol.* 18: 321–329.
52. Hakomori, S. 2003. Structure, organization, and function of glycosphingolipids in membrane. *Curr. Opin. Hematol.* 10: 16–24.
53. Fukuda, M. N., A. Dell, J. E. Oates, P. Wu, J. C. Klock, and M. Fukuda. 1985. Structures of glycosphingolipids isolated from human granulocytes. The presence of a series of linear poly-N-acetyllactosaminylceramide and its significance in glycolipids of whole blood cells. *J. Biol. Chem.* 260: 1067–1082.
54. Brackman, D., F. Lund-Johansen, and D. Aarskog. 1995. Expression of leukocyte differentiation antigens during the differentiation of HL-60 cells induced by 1,25-dihydroxyvitamin D3: comparison with the maturation of normal monocytic and granulocytic bone marrow cells. *J. Leukoc. Biol.* 58: 547–555.
55. Symington, F. W., I. D. Bernstein, and S. Hakomori. 1984. Monoclonal antibody specific for lactosylceramide. *J. Biol. Chem.* 259: 6008–6012.
56. Fujita, A., J. Cheng, M. Hirakawa, K. Furukawa, S. Kusunoki, and T. Fujimoto. 2007. Gangliosides GM1 and GM3 in the living cell membrane form clusters susceptible to cholesterol depletion and chilling. *Mol. Biol. Cell* 18: 2112–2122.
57. Iwabuchi, K., K. Handa, and S. Hakomori. 1998. Separation of "glycosphingolipid signaling domain" from caveolin-containing membrane fraction in mouse melanoma B16 cells and its role in cell adhesion coupled with signaling. *J. Biol. Chem.* 273: 33766–33773.
58. Iwabuchi, K., A. Prinetti, S. Sonnino, L. Mauri, T. Kobayashi, K. Ishii, N. Kaga, K. Murayama, H. Kurihara, H. Nakayama, et al. 2008. Involvement of very long fatty acid-containing lactosylceramide in lactosylceramide-mediated superoxide generation and migration in neutrophils. *Glycoconj. J.* 25: 357–374.
59. Luo, H. R., and F. Loison. 2008. Constitutive neutrophil apoptosis: mechanisms and regulation. *Am. J. Hematol.* 83: 288–295.
60. Green, D. R. 1998. Apoptotic pathways: the roads to ruin. *Cell* 94: 695–698.
61. Algeciras-Schimnich, A., L. Shen, B. C. Barnhart, A. E. Murmann, J. K. Burkhardt, and M. E. Peter. 2002. Molecular ordering of the initial signaling events of CD95. *Mol. Cell. Biol.* 22: 207–220.
62. Kayestha, R., A. Berry, and K. Hajela. 1993. Studies on a glucose-binding lectin from peripheral blood lymphocytes. *Immunol. Lett.* 38: 201–205.
63. Taylor, M. E., K. Bezouska, and K. Drickamer. 1992. Contribution to ligand binding by multiple carbohydrate-recognition domains in the macrophage mannose receptor. *J. Biol. Chem.* 267: 1719–1726.
64. Payne, C. M., L. Glasser, M. E. Tischler, D. Wyckoff, D. Cromey, R. Fiederlein, and O. Bohnert. 1994. Programmed cell death of the normal human neutrophil: an in vitro model of senescence. *Microsc. Res. Tech.* 28: 327–344.